Corrigendum to "Mare basalt meteorites, magnesian-suite rocks and KREEP reveal loss of zinc during and after lunar formation" [Earth Planet. Sci. Lett. 531 (2020) 115998]

James M.D. Day, Elishevah M.M.E. van Kooten, Beda Hofmann, Frédéric Moynier

Mare basalt meteorites, magnesian-suite rocks and KREEP reveal loss of zinc during and after lunar formation

James M.D Day[1,2*], Elishevah M.M.E. van Kooten[2], Beda A. Hofmann[3], Frederic Moynier[2]

[1]Scripps Institution of Oceanography, University of California San Diego, La Jolla, CA 92093-0244, USA

[2] Université de Paris, Institut de Physique du Globe de Paris, CNRS UMR 7154, Paris, France

[3]Naturhistorisches Museum Bern, Bernastrasse 15, CH-3005 Bern, Switzerland.

*Corresponding author: jmdday@ucsd.edu

Submitted to: *Earth and Planetary Science Letters*

Abstract: 369

Total Text: 6009

Figures: 7

Tables: 2

Supplementary Tables: 2

Keywords: Zinc; moon; magnesian-suite; KREEP; mare basalts; condensation; evaporation

Abstract

Isotopic compositions of reservoirs in the Moon can be constrained from analysis of rocks generated during lunar magmatic differentiation. Mare basalts sample the largest lunar mantle volume, from olivine- and pyroxene-rich cumulates, whereas ferroan anorthosites and magnesian-suite rocks represent early crustal materials. Incompatible element enriched rocks, known as 'KREEP,' probably preserve the last highly differentiated melts. Here we show that mare basalts, including Apollo samples and meteorites, have remarkably consistent δ^{66}Zn values (+1.4 ±0.2‰) and Zn abundances (1.5 ±0.4 ppm). Analyses of magnesian-suite rocks show them to be characterized by even heavier δ^{66}Zn values (2.5 to 9.3‰) and low Zn concentrations. KREEP-rich impact melt breccia Sayh al Uhaymir 169 has a nearly identical Zn composition to mare basalts (δ^{66}Zn = 1.3‰) and a low Zn abundance (0.5 ppm). Much of this variation can be explained through progressive depletion of Zn and preferential loss of the light isotopes in response to evaporative fractionation processes during a lunar magma ocean. Samples with isotopically light Zn can be explained by either direct condensation or mixing and contamination processes at the lunar surface. The δ^{66}Zn of Sayh al Uhaymir 169 is probably compromised by mixing processes of KREEP with mafic components. Correlations of Zn with Cl isotopes suggests that the urKREEP reservoir should be isotopically heavy with respect to Zn, like magnesian-suite rocks. Current models to explain how and when Zn and other volatile elements were lost from the Moon include *nebular processes*, prior to lunar formation, and *planetary processes*, either during giant impact, or magmatic differentiation. Our results provide unambiguous evidence for the latter process. Notwithstanding, with the currently available volatile stable isotope datasets, it is currently difficult to discount if the Moon lost its volatiles relative to Earth either during giant impact or exclusively from later magmatic differentiation. If the Moon did begin initially volatile-depleted, then the mare basalt δ^{66}Zn value likely preserves the signature, and the Moon lost 96% of its Zn

inventory relative to Earth and was also characterized by isotopically heavy Cl ($\delta^{37}Cl$ = ≥8‰). Alternative loss mechanisms, including erosive impact removing a steam atmosphere need to be examined in detail, but *nebular processes* of volatile loss do not appear necessary to explain lunar and terrestrial volatile inventories.

1. Introduction

Compared with Earth, the Moon is poor in volatile compounds (e.g., H_2O, CO_2) and elements (e.g., K, Na, Cl, Zn, Rb, Sn). Comparison of volatile element data for these planetary bodies shows that the Moon has lower ratios of element pairs that behave similarly during igneous processes but have a more volatile numerator over denominator, including K/U and Rb/Sr (e.g., Wolf & Anders, 1980; Jones & Palme, 2000; O'Neill and Palme 2008; Day & Moynier, 2014). The extent of volatile depletion, however, remains an open question. At one extreme, moderately volatile elements are depleted by a factor of ten or more (O'Neill, 1991; Albarede et al., 2015), whereas melt inclusions within olivine grains from the Apollo 74220 pyroclastic glass indicate that the Moon may have as much water as Earth's depleted upper mantle (Hauri et al., 2011; Ni et al., 2019). For the moderately volatile elements, defined by their nebular condensation temperatures intermediate between 'common' silicate minerals (forsterite, enstatite) and troilite (Lodders, 2003), stable isotope ratios are fractionated by evaporation/condensation processes (e.g., Herzog et al. 2009; Sharp et al., 2010; Paniello et al., 2012a; Kato et al., 2015; Boyce et al., 2015; Wang

74 & Jacobsen, 2016; Day et al., 2017a; 2019; Kato & Moynier, 2017; Pringle & Moynier, 2017;
75 Wang et al., 2019).

76

77 While the extent of volatile depletion in the Moon is an important question, how and when
78 volatile element depletion occurred may be even more critical. This is because the extent of volatile
79 depletion is dependent on how and when the process took place, which has 'planet-wide'
80 consequences. As noted previously (O'Neill and Palme 2008; Day & Moynier, 2014), at least two
81 phases of volatile depletion occurred during Solar System formation. The first was in the solar
82 nebula (*nebular depletion*), prior to or during the formation of the first solids. Partial or exclusive
83 loss of volatiles from the Moon has been proposed in this way (Humayun & Clayton, 1995; Taylor
84 el al., 2006). The second volatile depletion event, or series of events, is associated with
85 planetesimal and planet formation (*planetary depletion*). Within planetary depletion, there are
86 several avenues for volatile loss, focused around melting either during collisional events (Paniello
87 et al., 2012a; Kato & Moynier, 2017; Pringle & Moynier, 2017), or during differentiation of the
88 planets or planetesimals (Sharp et al., 2010; Kato et al., 2015; Boyce et al., 2015; Dhaliwal et al.,
89 2018).

90

91 One of the best-studied moderately volatile elements for examining volatile loss from the
92 Moon is zinc. Zinc has five stable isotopes, ^{64}Zn (48.6%), ^{66}Zn (27.9%), ^{67}Zn (4.1%), ^{68}Zn (18.8%)
93 and ^{70}Zn (0.6%) and the ^{66}Zn/^{64}Zn value is typically reported as the delta-notation (δ^{66}Zn =
94 ([(^{66}Zn/^{64}Zn)$_{sample}$/(^{66}Zn/^{64}Zn)$_{standard}$]-1) × 1000) relative to the 'Lyon' Zn standard, JMC 3–0749
95 L (see Moynier et al., 2017). Zinc is moderately volatile with a low 50% nebular condensation

96 temperature (~700K) and a low bond-bond energy (e.g., Lodders, 2003; Albarède et al., 2015).
97 Mass-dependent stable isotopic fractionation of an element occurs during any exchange reaction
98 and is due to the difference in vibrational energy of the bonds formed by the different isotopes at
99 equilibrium or to the difference of motions of the isotopes under kinetic conditions (e.g., Urey,
100 1947). Zinc has been measured in partial melt products from the lunar interior as mare basalts and
101 bulk pyroclastic glass beads, some ferroan anorthosites (FAN) that are considered to make up the
102 crust, and a few magnesian-suite (MGS) rocks, which are thought to be intrusions within the crust.
103 Data from these samples has revealed a range of δ^{66}Zn values in lunar samples, from -13.7‰ to
104 +6.4‰, which have been interpreted to reflect the various processes of volatile loss and
105 condensation, largely due to differentiation processes (Moynier et al., 2006; Herzog et al., 2009;
106 Paniello et al., 2012a; Kato et al., 2015; Day et al., 2017a).

107

108 There are some restrictions in the existing lunar Zn isotope dataset that limits interpretation of
109 how, when and to what extent volatile depletion occurred in the Moon. First, only two MGS rocks
110 have been examined (dunite 72415 and norite 77215), and they both exhibit heavy δ^{66}Zn values
111 (Kato et al., 2015), making analysis of further samples to examine whether this is a ubiquitous
112 signature of the MGS important. Alternatively, it is possible that the MGS could show similar
113 ranges in δ^{66}Zn to the FAN (Kato et al., 2015). Second, Apollo 11, 12, 15 and 17 mare basalts have
114 been examined from the Moon, but these are all near-side samples from a restricted area. Mare
115 basalt meteorites are considered to come from different regions of the Moon compared with the
116 Apollo samples (e.g., Korotev, 2005), so analysis of these samples is important for assessing the
117 likelihood of homogeneity of δ^{66}Zn in lunar mantle source regions. Finally, no potassium-rare
118 earth element-phosphorous enriched samples (KREEP) have been examined for Zn isotopes. This

is an important lunar reservoir, as it represents the dregs of magmatic differentiation, likely from a global magma ocean (Warren & Wasson, 1979). The δ^{66}Zn composition of KREEP would therefore constrain models of volatile loss during magma ocean crystallization processes. In this study, we take advantage of a new Zn isotopic method that decreases the required sample size by a factor of approximately ten to analyze the isotope and abundance data for four MGS rocks (15445 cataclastic anorthositic norite [CAN] clast, 15455 'B' norite clast, 78235 shocked norite, 76535 troctolite), four low-Ti (<4 wt.% TiO_2) mare basalt meteorites (La Paz 02205, Northwest Africa [NWA] 8632, NWA 479 and NWA 4734), as well as the first reported data on a KREEP-rich sample; the impact melt breccia of Sayh al Uhaymir [SaU] 169. With these data, we examine the loss of volatile Zn during processes acting prior to and during lunar formation.

2. Methods

Aliquots of powdered samples (50 to 250 mg) were digested in a mixture of ultra-pure HF/HNO_3 in Teflon beakers for 48 hours on a hotplate at 140°C. The samples were then dried down and Aqua Regia was added to dissolve the aliquots for another 24 hours on the hotplate. Zinc purification was achieved using an improved and miniaturized anion-exchange chromatography method, with a recovery of 99.99% (see Van Kooten & Moynier, 2019 for details). Samples (5 mg aliquots of total sample solutions) were loaded in 1.5N HBr on 0.1 ml AG-1X8 (200-400 mesh) ion-exchange columns and Zn was collected in 0.5N HNO_3. This purification step was repeated to ensure purification of the Zn fraction. The procedural blank measured with samples was 0.2 ng, and generally represents less than 4% of total measured Zn for samples, which was typically 5-10 ng (Van Kooten & Moynier, 2019). Zinc isotopic compositions were measured on the *Thermo Fischer* Neptune Plus multi collector-inductively coupled plasma-mass spectrometer housed at the

142 Institut de Physique du Globe, Paris. The Faraday cups were positioned to collect ions on the
143 masses 62, 63, 64, 65, 66, 67 and 68. Possible ^{64}Ni isobaric interferences were controlled and
144 corrected by measuring the intensity of the ^{62}Ni peak. A solution containing 10 ppb Zn in 0.1 M
145 HNO_3 was prepared for isotopic analysis. Isotopic ratios of Zn in all samples were analyzed using
146 an Apex IR introduction system, combined with a 100 µl/min PFA nebulizer. One block of 30
147 ratios, in which the integration time of 1 scan was 8.3 seconds, was measured for each sample.
148 The background was corrected by subtracting the on-peak zero intensities from a blank solution.
149 The instrumental mass bias was corrected by bracketing each of the samples with standards.

150

151 **3. Results**

152 Zinc isotope and abundance data for mare basalt meteorites (La Paz 02205, Northwest Africa
153 [NWA] 479, NWA 4734 and NWA 8632) spans a remarkably limited range, with 0.59 ±0.01 ppm
154 Zn and δ^{66}Zn of 1.23 ±0.05‰ (**Tables 1** and **2**). These values are more restricted than the range of
155 zinc abundance and isotopic compositions for Apollo mare basalts (δ^{66}Zn = +1.9 to -5.4‰; Zn =
156 0.6 to 12.1 ppm), although mare basalts typically fall within a restricted range of δ^{66}Zn
157 compositions (**Figure 1**). Compared with bulk pyroclastic glass bead data, the Apollo mare basalts
158 and mare basalt meteorites are typically isotopically heavier with respect to Zn and have lower
159 abundances.

160

161 The Apollo magnesian-suite (MGS) rocks span a limited range of Zn concentrations (0.42 to
162 1.36 ppm), and are all isotopically heavy (δ^{66}Zn = 2.46 to 9.27‰), confirming previous data
163 showing that crustal rocks have the heaviest isotope compositions of Zn of all lunar igneous rocks

(Kato et al., 2015). Similarly, high δ^{66}Zn has been measured in ferroan anorthosite 15415, with the other FAN samples that have been measured being isotopically light (**Fig. 1**). The MGS rocks examined in this study have been shown to be 'pristine', or free from impactor contamination (Gros et al., 1976; Warren et al., 1980; Day et al., 2010), despite the evidence for cataclasis in some MGS rocks (15445, as well as 77215 and 74215). The degree of shock and cataclasis of samples is not correlated with either Zn concentration or isotopic composition.

We analyzed a portion of the 3.91 ± 0.01 Ga mafic impact melt breccia lithology of Sayh al Uhaymir (SaU) 169 (Gnos et al., 2004). The ejection origin of this meteorite on the Moon has been attributed to the Procellarum KREEP terrane based on enrichments of Th (32.7 ppm), U (8.6 ppm) and K_2O (0.54 wt.%) within it, and it is the most KREEP-rich lunar sample examined to date (Gnos et al., 2004). Our analysis of Zn (0.47 ppm) and δ^{66}Zn (1.30 ± 0.04‰) are essentially identical to values obtained for the lunar mare basalt meteorites.

4. Discussion

4.1 Evaporation, condensation, mixing and contamination at the lunar surface

Lunar materials from the Apollo missions and as meteorites have been shown to form from the same silicate reservoirs based on stable isotopes of refractory major rock-forming elements (e.g., O, Mg, Si, Fe; Spicuzza et al., 2007: Liu et el., 2010; Armytage et al., 2012; Sossi & Moynier, 2017; Sedaghatpour & Jacobsen, 2019). For moderately volatile elements like zinc, the isotopic compositions of lunar crustal samples reflect effects of evaporation, condensation, mixing and contamination at the lunar surface (Moynier et al., 2006; Herzog et al., 2009; Paniello et al., 2012a;

186 Kato et al., 2015; Day et al., 2017a), as well as the Zn-bearing phases present in samples. For the
187 MGS rocks and FAN 15415, evaporation of isotopically light zinc from their parental melts that
188 exceeded those for mare basalt parental melts is required to explain both the low Zn contents and
189 high δ^{66}Zn (>2.5‰) of these samples. This process differs from that which formed the Zn-rich
190 (>10 ppm) regolith and regolith breccias, where impact gardening and spallation of isotopically
191 light Zn occurred over >100 Ma in the lunar surface environment (Moynier et al. 2006; Herzog et
192 al., 2009) (**Fig. 2**). Prior work has shown that evaporation processes during a magma ocean
193 operating throughout much/all of the Moon offers the most likely explanation for variable Zn (and
194 other volatile element) losses in magmatically-derived rocks (e.g., Day & Moynier, 2014; Boyce
195 et al., 2015; Dhaliwal et al., 2018).

196

197 Modelling the effect of zinc isotope evaporation is possible through empirically derived
198 fractionation factors that are closer to unity (>0.999) than theoretical values (Day et al., 2017b;
199 Wimpenny et al., 2019). Acknowledging that there was no single mantle source for MGS rocks,
200 we take the approach of modelling evaporation processes in them as a unified process, with an
201 initial starting composition of 30 ppm Zn and δ^{66}Zn = 1.25‰. The δ^{66}Zn was chosen to reflect a
202 source similar to the mare basalt source (e.g., Paniello et al., 2012a). The high content of Zn in the
203 source of MGS rocks is due to the progressive Zn enrichment that counters loss through
204 evaporation and that was likely to have occurred in a magma ocean (Dhaliwal et al., 2018). The
205 bulk partition coefficient for Zn under terrestrial conditions is typically approximated as close to
206 unity ($D_{mantle\text{-}melt}$~1), with limited fractionation of Zn isotopes during fractional crystallization
207 (e.g., Chen et al., 2013; Doucet et al., 2016), indicating that MGS rocks should derive from a
208 mantle reservoir that is more Zn-rich than for the mare basalts. The low Zn measured in mare

basalts (1-2 ppm) are consistent with previous estimates of a bulk Moon Zn content (~2 ppm; O'Neill, 1991). The choice of Zn concentration in the source is difficult to estimate without knowing the lunar bulk partition coefficient, but any concentration between ~10 and 30 ppm for the MGS parental melts leads to broadly similar outcomes to the models shown in **Figure 2**. However, higher estimated concentrations in the source (>30 ppm) or lower δ^{66}Zn (e.g., 0.3‰ as in chondrites or Earth) require lower fractionation factors and a poorer fit to the data.

The variable δ^{66}Zn of MGS rocks implies inhomogeneous evaporative loss of zinc amongst these samples, either reflecting different extents of evaporation, varying efficiency of evaporative fractionation, or heterogeneous initial Zn in their parental sources. These results are consistent with more than one mantle source of MGS samples, and for the possibility of mixing between early LMO olivine, plagioclase and KREEP reservoirs (e.g., Shearer et al., 2015). The variability in Zn isotopic compositions in the MGS rocks and in FAN 15415 are most consistent with inheritance of these signatures from variable evaporative loss during the late stages of a magma ocean, and after formation of the mare basalt source reservoirs, where higher δ^{66}Zn values are expected provided that the resultant evaporated Zn condensates could be effectively lost (Dhaliwal et al., 2018). The CAN clast of 15455 (9.3‰), cataclastic dunite 72415 (6.3‰) and 15415 (4.2‰) would represent products from the most extremely fractionated and latest crystallized melts in this model.

Some of the isotopically light condensate Zn from lunar degassing remains on the lunar surface today. Analysis of the 'Rusty Rock' 66095 has illustrated how magmatic outgassing, during

impact-related or volcanic events on the Moon, led to significant condensation of isotopically light vapors into the impact melt breccia (Day et al., 2017a; 2019). Similarly, volatile condensation onto the lunar surface can explain how late-stage differentiates in the Moon evolved to higher δ^{66}Zn than mare basalt sources. Modelled condensate compositions match δ^{66}Zn values measured for the Zn-rich 'Rusty Rock' 66095 (**Fig. 2**). Mixing of evaporated reservoirs and condensates on the lunar surface also matches trends observed in δ^{66}Zn and Zn content for the FAN, further reinforcing the concept that volatile loss during the magma ocean was facilitated by the formation of the lunar crust. Stabilization and thickening of the cooling lunar crust would inevitably have led to the formation of a sink for condensate volatiles, separating them from the magma ocean, and enabled rapid depletion of volatile contents in the hot molten rocks, without the requirement for other volatile-loss mechanisms.

4.2 Zinc isotope composition of mare basalt sources

With five exceptions (10017, 12005, 12018, 14053, 15016), mare basalts have a range of δ^{66}Zn values from 0.8 to 1.9‰ (**Fig. 3**). As originally suggested by Paniello et al. (2012a) and quantified in the presented models, mixing and contamination from isotopically light Zn on the lunar surface explains the isotopically light basalts reported previously. Mixing and contamination of between 10 and 50% condensate Zn matching that measured in 66095 provides a good approximation for the Zn compositions of these anomalous mare basalts. These results are supported by leaching experiments on 14053 which show that the silicate fraction of the sample was identical to the majority of mare basalts at ~1.4‰ (Day et al., 2017a). Contamination of lunar mare basalts could have occurred through two mechanisms. First, Zn could have been assimilated during ascent of

253 magmas and eruption on the lunar surface, where mare basalts would be highly sensitive to
254 assimilation of volatile phases due to low magmatic Zn contents (<2 ppm) versus high contents in
255 condensates (e.g., 300 ppm in 66095). Second, Zn addition could have occurred through partial
256 condensation directly onto samples during or after they had crystallized. This latter process is
257 possibly analogous to the pyroclastic glass beads 15426, 74001 and 74220, that experienced
258 directed condensation onto the bead surfaces, during or after their formation. The surface areas of
259 the beads, combined with evidence for Zn phases on the exteriors of the beads (Ma & Liu, 2019)
260 and high Zn abundances correlated to these outer surfaces (e.g. Herzog et al. 2009), implies that
261 the beads were effective 'traps' of condensate volatile species.

262

263 It has been suggested that volatile loss of Cl occurred during eruption and crystallization of
264 lava flows on the lunar surface (Sharp et al., 2010). To examine whether Zn isotopes were
265 fractionated during eruption, we compare mare basalt δ^{66}Zn values with petrological proxies of
266 outgassing and lava-flow differentiation. We compare texture, presence or absence of vesicles and
267 vugs, and bulk-rock MgO content. The presence of vesicles in basaltic rocks indicates outgassing
268 of gas species, while coarser-grained lava samples might be associated with prolonged outgassing
269 processes at the lunar surface, or relate to suites of samples from the Apollo landing sites
270 originating from the same lava flow. Magnesium oxide (MgO) is an indicator of differentiation, as
271 this compound is compatible in early crystallizing silicate mineral phases, including olivine,
272 orthopyroxene and clinopyroxene. Relationships of MgO with Zn and δ^{66}Zn, therefore, might be
273 expected to relate to outgassing prior to, during and after eruption during lava flow differentiation
274 processes in Apollo mare basalt suites (e.g., Rhodes & Hubbard, 1973; Neal & Taylor, 1992;
275 Schnare et al., 2008). While some mare basalt samples, specifically some of the mare basalt

meteorites, have quantitative textural data associated with them (Day & Taylor, 2007), textural descriptions in the literature for Apollo mare basalts are often qualitative, being described as fine, medium or coarse grained. Mare basalt samples also have a range of textures from porphyritic (e.g., 15058, 15499), to poikilitic (e.g., 70135), ophitic or aphanitic. Acknowledging current petrological complexities, we defined samples where average grain sizes are reported as <0.5 mm as fine-grained, samples with grain sizes of >2 mm as coarse grained, and intermediate samples as medium-grained (**Table S1**).

Comparison of δ^{66}Zn with presence or absence of vesicles shows that they are not correlated (**Fig. 4**). Mare basalts with the most negative δ^{66}Zn (<-1‰) are medium to fine-grained, but otherwise there is no relationship of grain-size with mare basalt δ^{66}Zn values. Nor do the Zn isotope compositions track changes with magmatic differentiation. Low-Ti mare basalts have uniformly low Zn abundances (<2 ppm) and there is no correlation between MgO and δ^{66}Zn (**Fig. 5**). High-Ti basalts show a wide range of δ^{66}Zn and Zn content for a limited range of MgO, likely due to higher compatibility of Zn within spinel and oxide phases, but otherwise no relationships between δ^{66}Zn and MgO exist. While these lines of evidence do not rule out minor degassing of Zn during lava flow emplacement processes, or for degassing of other volatiles, such as H or Cl, they demonstrate that this is not the dominant process for δ^{66}Zn variations in mare basalts. Instead, these comparisons provide evidence that the average δ^{66}Zn of mare basalts reflect that of their mantle source reservoirs within the Moon, as suggested previously (Paniello et al., 2012a; Kato et al., 2015). We confirm this with new mare basalt meteorite data that suggest a homogeneous mare basalt mantle source reservoir for zinc. Removing the five samples with negative δ^{66}Zn from the

298 compilation, mare basalts as a whole are characterized by a δ^{66}Zn value of 1.40 ± 0.08‰ (**Table**
299 **2**). There are variations in δ^{66}Zn between high-Ti mare basalts (1.50 ±0.15‰) and low-Ti mare
300 sources (1.37 ±0.15‰), but any significant differences that may occur are outside current levels
301 of analytical precision.

302

303 ***4.3 The zinc isotope composition of KREEP and relations to H and Cl***

304 The potassium-rare earth element-phosphorous enriched (KREEP) reservoir has been shown
305 to exist dominantly in the nearside Procellarum KREEP Terrane (Jolliff et al., 2000). Numerous
306 Apollo 12 and 14 samples, MGS rocks, and some mare basalt meteorites (e.g., LaPaz mare basalts)
307 have KREEP signatures and similar inter-element ratios of incompatible elements, implying a
308 single KREEP reservoir, sometimes referred to as urKREEP (Warren & Wasson, 1979). This
309 reservoir is postulated to have formed during crystallization of a lunar magma ocean, where
310 elements that are incompatible in silicate minerals (olivine, pyroxene, plagioclase) would be
311 predicted to concentrate in residual melts. Given that many moderately volatile elements and
312 compounds like water are incompatible, this reservoir should be the most volatile-rich reservoir in
313 the Moon. This appears to be the case for Cl, which is estimated to have ~28 times higher
314 abundances relative to mare basalts (Boyce et al., 2018).

315

316 To date, no pristine urKREEP sample has been discovered, and all KREEP-rich rocks have
317 Mg-numbers (atomic ratios of Mg/Mg + Fe) too high to have formed as direct late-stage magma
318 ocean products (e.g., Snyder et al., 1992). KREEP-rich rocks with high Mg-numbers can be
319 explained by the incorporation of an urKREEP signature, via mixing or contamination, into partial

320 melts from early-formed olivine and pyroxene-rich cumulate reservoirs (e.g., Warren & Wasson,
321 1979; Snyder et al., 1992; Shearer et al., 2015). The SaU 169 impact melt breccia is no exception
322 to this rule; while it is among the most KREEP-rich samples reported to date, being enriched in
323 incompatible trace elements by factors of 1.5 to 1.8 relative to the KREEP composition reported
324 by Warren & Wasson (1979), it is also Mg-rich (Mg-number = 70; Gnos et al., 2004). SaU 169
325 has similar Zn isotope and abundance systematics to mare basalts (**Table 1**); this differs from the
326 prediction that KREEP should be heavier for δ^{66}Zn based on models of magma ocean processes
327 (Dhaliwal et al., 2018). We suggest two possible reasons for this discrepancy and favor the latter
328 explanation. First, the similarity of δ^{66}Zn in KREEP compared with mare basalts could reflect no
329 change in δ^{66}Zn during magma ocean processes, contrary to models. Second, the δ^{66}Zn of SaU 169
330 is not reflective of pure urKREEP, but is rather reflective of mixing with mafic components during
331 its petrogenesis.

332

333 Boyce et al. (2015) and Barnes et al. (2016) have argued for KREEP mixing into mare basalt
334 sources to explain apatite δ^{37}Cl values, and have made this association from extrapolations with
335 MGS rocks, including 76535 and 78235, which are isotopically heavy with respect to Cl (δ^{37}Cl =
336 >30‰) and that have fractionated La/Lu and La/Sm, consistent with an urKREEP signature. These
337 MGS samples also have high δ^{66}Zn (3.1 to 3.5‰), so if KREEP was partially responsible for the
338 variations in moderately volatile isotopic compositions, one might also expect to see a correlation
339 with Zn isotopes in mare basalts and a KREEP signature. Abundance ratios of La and Lu are useful
340 for assessing possible urKREEP mixing with mare basalts, because urKREEP is considered to
341 have high La (230 ppm) and Lu (7.8 ppm), with La/Lu of 29.5, versus KREEP-free mare sources
342 with lower La (1.1 ppm) and Lu (0.26 ppm) and a low La/Lu ratio (4.2) (Boyce et al., 2018). Mare

343 basalt La/Lu ratios are not correlated with Zn isotopic composition (**Table S1**), with Apollo 17
344 basalts with low La/Lu (~4) having broadly similar δ^{66}Zn to Apollo 15 basalts with the highest
345 La/Lu (~18). This result indicates that admixtures of KREEP and a mare basalt source are not
346 required to explain δ^{66}Zn values in mare basalts. Consequently, this suggests that KREEP addition
347 does not control Zn isotopic variations in mare basalts, or that KREEP has the same δ^{66}Zn value
348 to the mare basalt source.

349

350 In contrast, evidence supporting a higher δ^{66}Zn value for KREEP than that measured in SaU
351 169 comes from comparisons of Zn with H and Cl isotope compositions. Comparison of Zn with
352 Cl and H is not intuitive as H and Cl abundances tend to be measured within apatite, where they
353 can be preferentially partitioned into the mineral structure ($Ca_5[PO_4]_3[Cl,F,OH]$), whereas Zn is
354 likely sited within S-rich phases and silicate minerals in lunar rocks. Indeed, analysis of the Rusty
355 Rock, 66095, has demonstrated decoupling of Cl, Cu and Fe from Zn isotope compositions, largely
356 due to condensation effects on the sample (Day et al., 2017a; 2019). In contrast, magmatic phases
357 are likely to trap the H, Cl and Zn compositions within mare basalts and HMS rocks making
358 comparisons between these elements possible. Positively correlated relationships for Cl and Zn
359 have previously been reported for eucrite meteorites (Sarafian et al., 2017; Barrett et al., 2019).
360 This trend has been interpreted to reflect degassing of $ZnCl_2$ in an H-poor environment in the
361 eucrite parent body (4 Vesta).

362

363 We find no relationship between H and Zn isotope ratios (**Fig. 6a**). However, we note a
364 relationship of increasing δ^{37}Cl with increasing δ^{66}Zn from mare basalts to MGS rocks (**Fig. 6b**).

The Zn-Cl isotope lunar trend is not well-developed and is steeper than the eucrite data trend. For a given Cl isotope composition, Zn isotopes are less fractionated in lunar samples than in eucrite meteorites, implying possible differences in extents and style of degassing. Furthermore, for mare basalts, there is a restricted range in Zn ($\delta^{66}Zn$ = 1.4‰), as well as consistently heavy Cl isotope compositions ($\delta^{37}Cl$ = 8 to 15‰). KREEP impact melt breccia SaU 169 lies within this range ($\delta^{66}Zn$ = 1.3‰, $\delta^{37}Cl$ = 9‰). This composition likely reflects the dominant role of a mafic component in the sample, consistent with the high MgO (12.2 wt.%) and bulk composition of the impact melt breccia itself (Gnos et al., 2004).

The most extremely heavy $\delta^{66}Zn$ from the Moon is for the CAN clast in 15455 (9.3‰), versus for basaltic eucrite DaG 945 (13.5‰) that is the most extreme equivalent from Vesta. These comparisons suggest that greater loss of Zn occurred on Vesta compared with the Moon, which would confirm previous measurements of K/U and Rb/Sr ratios, and with planetary body size (Day & Moynier, 2014). Estimates for maximum chlorine loss via degassing are similar for the Moon and Vesta (**Fig. 6**), which makes this isotope proxy of moderately volatile element loss distinct from those of $\delta^{66}Zn$, K/U or Rb/Sr. These results suggest contrasting degassing processes for Cl and Zn, with Zn loss on Vesta possibly occurring as $ZnCl_2$ (e.g., Barrett et al., 2019). The lunar urKREEP composition is an important composition to measure for Zn isotopes to examine volatile loss models for Moon and Vesta. Based on KREEPy impact breccia SaU 169, the KREEP reservoir would have δD, $\delta^{37}Cl$ and $\delta^{66}Zn$ within the range of mare basalts, but these values are significantly lower in δD and $\delta^{37}Cl$ than for the classic KREEP basalt 15382/6. Magma ocean models predict urKREEP to have $\delta^{66}Zn$ higher than mare basalt sources (Dhaliwal et al., 2018). To test if KREEP

387 does have an elevated Zn isotope composition, and if degassing processes on Vesta and Moon
388 were similar, measurement of KREEP basalt 15382/6 will be critical given the high $\delta^{37}Cl$ (22
389 ±8‰; Barnes et al., 2016) of apatite grains within the sample.

390

391 ### *4.4 Early loss of Zn and Cl through crust-breaching impacts or before lunar formation?*

392 The significant difference between $\delta^{66}Zn$ values of MGS rocks and mare basalts provide
393 unequivocal evidence that Zn was lost, and its isotopes fractionated, during evaporative
394 fractionation processes on the Moon. The most likely cause of Zn loss between the formation of
395 the mare basalt sources and the crystallization of MGS rocks was during magma ocean
396 differentiation, supporting models of progressive loss of volatiles from the lunar interior during
397 magma ocean degassing (Dhaliwal et al. 2018), and the elevated $\delta^{66}Zn$ and $\delta^{35}Cl$ values in MGS
398 rocks. On the other hand, the homogenous $\delta^{66}Zn$ values of mare basalt sources suggest a large-
399 scale process for their generation, either through magma ocean processes (Kato et al., 2015;
400 Dhaliwal et al., 2018), or prior to or during the giant impact (Paniello et al., 2012a). The bulk
401 silicate Earth (BSE) value for $\delta^{66}Zn$ is between 0.16 and 0.3‰ (Chen et al., 2013; Wang et al.,
402 2017; Sossi et al., 2018), and its Zn content is estimated at 55 ppm (McDonough & Sun, 1995),
403 whereas the $\delta^{66}Zn$ and Zn content for CI chondrites are ~0.3‰ and 310 ppm (Moynier et al., 2017).
404 As mentioned previously, mare basalt sources have $\delta^{66}Zn$ of 1.40 ± 0.08‰, and Zn contents as
405 low as 1-2 ppm. At face value, the BSE is depleted by more than 80% of Zn compared with
406 chondrites, assuming it formed from similar sources, without significantly fractionating Zn
407 isotopes. Part of the BSE Zn loss can be explained by core formation as under conditions relevant
408 to Earth's core differentiation Zn is slightly siderophile and the bulk Earth may have ~ 114 ppm

409 (Mahan et al. 2017). Conversely, the reservoir of mare basalts has lost significantly more Zn (99%
410 relative to chondrites, 96% relative to Earth), and has experienced evaporative fractionation of Zn
411 isotopes, suggesting that the lunar Zn depletion is due to planetary processes.

412

413 Understanding whether the difference in Zn abundances and isotopic compositions between
414 the Moon and Earth occurred through volatile-loss of material forming the Moon in a giant impact
415 (**Fig. 7**), or whether it was wholly lost after this event during magma ocean degassing and other
416 processes on the Moon, is important for models to explain the formation of the Moon, including
417 volatile loss during a lunar 'synestia' (Lock et al., 2018), from a lunar disk (Nakajima & Stevenson,
418 2018), or from the Moon itself (Dhaliwal et al. 2018). Dhaliwal et al. (2018) showed that during
419 magma ocean processes, volatile loss could occur throughout the cooling of the magma ocean, but
420 that the volatile condensates required a loss-mechanism. The 'problem' of how to separate
421 isotopically light condensate Zn from the melt residue during magma ocean processes on the Moon
422 can be at least partially resolved by condensation onto the cooling lunar surface (Day et al., 2017a),
423 or to the Earth when the early forming Moon was at the Roche limit (Sossi et al. 2018).
424 Condensation of volatiles on the forming crust acts to effectively remove the isotopically light Zn
425 condensate and would indicate that Zn isotope fractionation might have been initially slow during
426 the early stages of lunar differentiation when early-formed crust as only semi-permanent,
427 foundering into the lunar interior. Later, as the crust became stable and permanent, rapid evolution
428 and complexity in Zn isotope compositions of crustal rocks could have occurred.

429

Another likely mechanism for volatile loss might include impacts to the Moon during lunar magma ocean formation and after dissipation of a nascent atmosphere surrounding the Moon (**Fig. 7**), as has been suggested previously (Barnes et al., 2016). Retention of impactor mass has been shown to be quite low, of the order of 20 to 30%, and large impactors striking the Moon were likely to have been numerous, with as many as 300 impact basins of initial diameters of 300 km or more up to ~4.1 Ga (Zhu et al., 2019). These features imply that erosive-loss of a nascent atmosphere on the Moon was likely and may have occurred as many as 300 times or more between the formation of the Moon and ~4.1 Ga. However, the likelihood of erosive loss of isotopically light condensates from the Moon is limited for two reasons. First is the effectiveness and quantity of volatile species that can be retained as a steam gas atmosphere above a molten magma ocean on the Moon, prior to erosive impacts. Second, is the requirement that loss of Zn by impact erosion must have affected the Moon across the entire formation of mare basalt sources, from low-Ti to high-Ti compositions, during a magma ocean (**Fig. 7**). To fully investigate this problem, combined modeling efforts to estimate gas contents in a lunar steam atmosphere and to examine if impact-erosion can successfully remove this atmosphere are needed.

Alternatively, the homogeneity of mare basalt δ^{66}Zn values might suggest a global signature of volatile element depletion inherited from the giant impact. Various studies have proposed loss of moderately volatile elements (K, Rb, Ga, Sn: Wang & Jacobson, 2016; Pringle & Moynier, 2017; Kato & Moynier, 2017; Wang et al., 2019) prior to the formation of the Moon, but few of them have been able to provide robust resolution of when volatile loss occurred, mainly due to the limited number of samples and associated lunar reservoirs analyzed. Arguments have typically relied on differences in the isotopic compositions of moderately volatile elements between lunar

453 and terrestrial samples. However, this approach cannot necessarily discriminate between volatile
454 element loss prior to the formation of the Moon, from nebular volatile loss processes, during giant
455 impact, or during or after the formation of the Moon.

456

457 With a large set of Zn isotope data it is possible to distinguish processes acting on volatile
458 elements *after* the formation of the Moon. The heavy δ^{66}Zn (>2.5‰) of pristine MGS and FAN
459 samples, and the light isotopic compositions of some mare basalts and FAN (<0‰) can be
460 explained by magmatic degassing and condensation of isotopically light Zn, respectively. If the
461 Moon did experience moderately volatile element loss *prior to*, or *during* its formation, then the
462 Zn isotope signature of that event would be recorded by the mare basalts at 1.4‰. In this scenario,
463 significant moderately volatile element loss and Zn isotope fractionation occurred to materials
464 forming the Moon, leading to a 1.1 to 1.2‰ difference between terrestrial δ^{66}Zn (~0.16-0.3‰;
465 Chen et al., 2013; Wang et al., 2017; Moynier et al. 2017; Sossi et al., 2018) and the composition
466 of the Moon. Without data for urKREEP to examine the maximum extents of magma ocean
467 degassing, and without collision models to examine if volatile elements could be effectively
468 stripped from the Moon during its formation, it is impossible to say with confidence if this
469 signature was inherited *prior to*, *during* or *after* the formation of the Moon. Notwithstanding, if
470 mare basalts do record the Zn isotope signature during the formation of the Moon, then it would
471 suggest that the Moon also inherited an isotopically heavy Cl (δ^{37}Cl = 8 to 15‰) signature from
472 this event.

473

474 **5. Conclusions and implications for volatile loss during moon and planet formation**

475 New data are presented for mare basalt meteorites to show that they, and Apollo mare basalts,
476 have remarkably consistent δ^{66}Zn values (+1.4 ±0.2‰) and low Zn (1.5 ±0.4 ppm) inherited from
477 their mantle sources. New analyses of magnesian-suite rocks show them to be characterized by
478 even heavier δ^{66}Zn values (2.5 to 9.3‰) and low Zn concentrations. Zinc isotope analysis of
479 KREEP impact melt sample Sayh al Uhaymir 169 shows that it has a nearly identical composition
480 to mare basalts (δ^{66}Zn = 1.3‰, 0.5 ppm [Zn]). We explain these variations through progressive
481 depletion of Zn and preferential loss of the light isotopes in response to evaporative fractionation
482 processes during lunar magmatic differentiation. Variations in δ^{66}Zn in samples to isotopically
483 light values can be explained by condensation of isotopically light Zn on the lunar surface and
484 mixing and contamination processes with magmas interacting with these surface reservoirs. The
485 δ^{66}Zn of KREEP defined by Sayh al Uhaymir 169 is likely to be compromised by mixing processes
486 with a mafic component. Correlations of Zn with Cl isotopes suggests that the KREEP reservoir
487 should also be isotopically heavy, like the magnesian-suite rocks, and analysis of 15382/15386
488 will be essential to test this hypothesis.

489

490 Current models to explain how and when Zn and other volatile elements were lost from the
491 Moon include *nebular processes*, prior to the Moon's formation, and *planetary processes*, either
492 during the formation of the Moon in a giant impact, or during magmatic differentiation. Our results
493 provide unambiguous evidence for the latter process and imply that *nebular processes* are not
494 required to explain the excessive depletion in volatile elements in the Moon relative to Earth. On
495 the other hand, with the currently available volatile stable isotope datasets, it is currently difficult
496 to say with certainty whether the Moon lost its volatiles relative to Earth either during giant impact
497 or from later magmatic differentiation. If the Moon did begin initially volatile-depleted, then the

498 mare basalt $\delta^{66}Zn$ value likely preserves that signature, in which case the Moon lost 96% of its
499 zinc inventory relative to Earth at that time and was also characterized by isotopically heavy Cl
500 ($\delta^{37/35}Cl = \geq 8‰$).

501

502 **Acknowledgements**

503 Constructive and helpful reviews by J. Barnes and an anonymous are gratefully acknowledged.
504 We thank the lunar subcommittee of NASA CAPTEM, and the Meteorite Working Group for
505 provision of Apollo and Antarctic meteorites, respectively. US Antarctic meteorite samples are
506 recovered by the Antarctic Search for Meteorites (ANSMET) program which has been funded by
507 NSF and NASA and characterized and curated by the Department of Mineral Sciences of the
508 Smithsonian Institution and Astromaterials Curation Office at NASA Johnson Space Center. SaU
509 169 was recovered during a joint Omani-Swiss search campaign supported by the Public Authority
510 for Mining, Sultanate of Oman, and the Swiss National Science Foundation. This work was
511 supported by the NASA Emerging Worlds program (NNX15AL74G) and an IPGP Visiting
512 Professor position to JD. FM acknowledges funding from the European Research Council under
513 the H2020 framework program/ERC grant agreement #637503 (Pristine), as well as financial
514 support of the UnivEarthS Labex program at Sorbonne Paris Cité (ANR-10-LABX-0023 and
515 ANR-11-IDEX-0005-02), and the ANR through a chaire d'excellence Sorbonne Paris Cité. EK
516 acknowledges funding from the European Union's Horizon 2020 research and innovation
517 programme under the Marie Skłodowska-Curie Grant Agreement No 786081.

518

519 **References**

520 Albarède, F., Albalat, E., Lee, C.T.A., 2015. An intrinsic volatility scale relevant to the Earth and
521 Moon and the status of water in the Moon. Meteoritics & Planetary Science 50, 568-577.
522 Armytage, R.M.G., Georg, R.B., Williams, H.M., Halliday, A.N., 2012. Silicon isotopes in lunar
523 rocks: implications for the Moon's formation and the early history of the Earth. Geochimica et
524 Cosmochimica Acta, 77, 504-514.
525 Barnes, J.J., Tartèse, R., Anand, M., McCubbin, F.M., Franchi, I.A., Starkey, N.A., Russell, S.S.,
526 2014. The origin of water in the primitive Moon as revealed by the lunar highlands samples.
527 Earth and Planetary Science Letters, 390, 244-252.
528 Barnes, J.J., Tartese, R., Anand, M., McCubbin, F.M., Neal, C.R., Franchi, I.A., 2016. Early
529 degassing of lunar urKREEP by crust-breaching impact(s). Earth and Planetary Science Letters,
530 447, 84-94.
531 Barnes, J.J., Franchi, I.A., McCubbin, F.M., Anand, M., 2018. Multiple reservoirs of volatiles in
532 the Moon revealed by the isotopic composition of chlorine in lunar basalts. Geochimica et
533 Cosmochimica Acta, https://doi.org/10.1016/j.gca.2018.12.032.
534 Barrett, TJ., Barnes, J.J., Anand, M., Franchi, I.A., Greenwood, R.C., Charlier, B.L.A., Zhao, X.,
535 Moynier, F., Grady, M.M., 2019. Investigating magmatic processes in the early Solar System

536 using the Cl isotopic systematics of eucrites. Geochimica et Cosmochimica Acta,
537 https://doi.org/10.1016/j.gca.2019.06.024
538 Boyce, J.W., Treiman, A.H., Guan, Y., Ma, C., Eiler, J.M., Gross, J., Greenwood, J.P., Stolper,
539 E.M., 2015. The chlorine isotope fingerprint of the lunar magma ocean. Science Advances, 1,
540 e1500380.
541 Boyce, J.W., Kanee, S.A., McCubbin, F.M., Barnes, J.J., Bricker, H., Treiman, A.H., 2018. Early
542 loss, fractionation, and redistribution of chlorine in the Moon as revealed by the low-Ti lunar
543 mare basalt suite. Earth and Planetary Science Letters, 500, 205-214.
544 Chen, H., Savage, P.S., Teng, F.-Z., Helz, R.T., Moynier, F., 2013. Zinc isotopic fractionation
545 during magmatic differentiation and the isotopic composition of the bulk Earth. Earth and
546 Planetary Science Letters, 369-370, 34-42.
547 Chen, Y., Zhang, Y., Liu, Y., Guan, Y., Eiler, J., Stolper, E.M., 2015. Water, fluorine, and sulfur
548 concentrations in the lunar mantle. Earth and Planetary Science Letters 427, 37-46.
549 Day, J.M.D., Taylor, L.A., 2007. On the structure of mare basalt lava flows from textural analysis
550 of the LaPaz Icefield and Northwest Africa 032 lunar meteorites. Meteoritics & Planetary
551 Science, 42, 3-17.
552 Day, J.M.D., Moynier, F., 2014. Evaporative fractionation of volatile stable isotopes and their
553 bearing on the origin of the Moon. Phil. Trans. Royal Soc. London A, 372(2024), 20130259.
554 Day, J.M.D., Walker, R.J., James, O.B., Puchtel, I.S., 2010. Osmium isotope and highly
555 siderophile element systematics of the lunar crust. Earth and Planetary Science Letters, 289,
556 595-605.
557 Day, J.M.D., Moynier, F., Shearer, C.K. 2017a. Late-stage magmatic outgassing from a volatile-
558 depleted Moon. Proceedings of the National Academy of Sciences, 114, 9457-9551.
559 Day, J.M.D., Moynier, F., Meshik, A.P., Pradivtseva, O.V. and Petit, D.R., 2017b. Evaporative
560 fractionation of zinc during the first nuclear detonation. Science advances, 3, e1602668.
561 Day, J.M.D., Sossi, P.A., Shearer, C.K., Moynier, F., 2019. Volatile distributions in and on the
562 Moon revealed by Cu and Fe isotopes in the 'Rusty Rock' 66095. Geochimica et Cosmochimica
563 Acta. https://doi.org/10.1016/j.gca.2019.02.036
564 Dhaliwal, J.K., Day, J.M.D., Moynier, F., 2018. Volatile element loss during planetary magma
565 ocean phases. Icarus, 300, 249-260.
566 Doucet, L.S., Mattielli, N., Ionov, D.A., Debouge, W., Golovin, A.V., 2016. Zn isotopic
567 heterogeneity in the mantle: A melting control? Earth and Planetary Science Letters, 451, 232-
568 240.
569 Gnos E., Hofmann B.A., Al-Kathiri A., Lorenzetti S., Eugster O., Whitehouse M.J., Villa I., Jull
570 A.J.T., Eikenberg J., Spettel B., Krähenbühl U., Franchi I.A., Greenwood R.C. (2004)
571 Pinpointing the source of a lunar meteorite: Implications for the evolution of the Moon. Science
572 305, 657-659.
573 Gros, J., Takahashi, H., Hertogen, J., Morgan, J.W., Anders, E., 1976. Composition of the
574 projectiles that bombarded the lunar highlands. Lunar and Planetary Science Conference
575 Proceedings, 7, 2403-2425.
576 Hauri, E. H.,Weinreich, T., Saal, A., Rutherford, M., Van Orman, J. A., 2011. High Pre-Eruptive
577 Water Contents Preserved in Lunar Melt Inclusions. Science, 333, 213-215.
578 Herzog, G.F., Moynier, F., Albarède, F., Berezhnoy, A.A., 2009. Isotopic and elemental
579 abundances of copper and zinc in lunar samples, Zagami, Pele's hairs, and a terrestrial basalt.
580 Geochimica et Cosmochimica Acta 73, 5884-5904.

581 Hui, H., Guan, Y., Chen, Y., Peslier, A.H., Zhang, Y., Liu, Y., Flemming, R.L., Rossman, G.R.,
582 Eiler, J.M., Neal, C.R., Osinski, G.R., 2017. A heterogeneous lunar interior for hydrogen
583 isotopes as revealed by the lunar highlands samples. Earth and Planetary Science Letters, 473,
584 14-23.
585 Humayun, M., Clayton, R.N., 1995. Potassium isotope geochemistry: genetic implications of
586 volatile element depletion. Geochimica et Cosmochimica Acta, 59, 2115-2130.
587 Jolliff, B.L., Gillis, J.J., Haskin, L.A., Korotev, R.L., Wieczorek, M.A., 2000. Major lunar crustal
588 terranes: Surface expressions and crust-mantle origins. Journal of Geophysical Research:
589 Planets, 105, 4197-4216.
590 Jones, J.H., Palme, H., 2000. Geochemical constraints on the origin of the Earth and Moon. In:
591 Canup, R.M., Righter, K. (Eds.) Origin of the Earth and Moon, University of Arizona Press,
592 Tucson, 555 pp., p.197-216.
593 Kato, C., Moynier, F., Valdes, M.C., Dhaliwal, J.K., Day, J.M.D., 2015. Extensive volatile loss
594 during formation and differentiation of the Moon. Nature communications, 6, 7617.
595 Kato, C., Moynier, F., 2017. Gallium isotopic evidence for extensive volatile loss from the Moon
596 during its formation. Science advances, 3, e1700571.
597 Korotev R. L., 2005. Lunar geochemistry as told by lunar meteorites. Chemie der Erde 65, 297-
598 346.
599 Liu, Y., Spicuzza, M.J., Craddock, P.R., Day, J.M.D., Valley, J.W., Dauphas, N., Taylor, L.A.,
600 2010. Oxygen and iron isotope constraints on near-surface fractionation effects and the
601 composition of lunar mare basalt source regions. Geochimica et Cosmochimica Acta, 74, 6249-
602 6262.
603 Lock, S.J., Stewart, S.T., Petaev, M.I., Leinhardt, Z., Mace, M.T., Jacobsen, S.B. and Cuk, M.,
604 2018. The origin of the Moon within a terrestrial synestia. Journal of Geophysical Research:
605 Planets, 123, 910-951.
606 Lodders, K., 2003. Solar System abundances and condensation temperatures of the elements.
607 Astrophysical Journal, 591, 1220-1247.
608 Ma, C., Liu, Y., 2019. Discovery of a zinc-rich mineral on the surface of lunar orange pyroclastic
609 beads. American Mineralogist, 104, 447-452.
610 McCubbin, F.M., Kaaden, K.E.V., Tartese, R., Klima, R.L., Liu, Y., Mortimer, J., Barnes, J.J.,
611 Shearer, C.K., Treiman, A.H., Lawrence, D.J., Elardo, S.M., 2015. Magmatic volatiles (H, C,
612 N, F, S, Cl) in the lunar mantle, crust, and regolith: Abundances, distributions, processes, and
613 reservoirs. American Mineralogist 100, 1668-1707.
614 McDonough, W.F., Sun, S.-S., 1995. The composition of the Earth. Chemical Geology, 120, 223-
615 254.
616 Moynier, F., Albarède, F., Herzog, G.F. 2006. Isotopic composition of zinc, copper, and iron in
617 lunar samples. Geochimica et Cosmochimica Acta 70, 6103–6117.
618 Moynier, F., Vance, D., Fujii, T., Savage, P., 2017. The isotope geochemistry of zinc and copper.
619 Reviews in Mineralogy and Geochemistry, 82, 543-600.
620 Nakajima, M. and Stevenson, D.J., 2018. Inefficient volatile loss from the Moon-forming disk:
621 Reconciling the giant impact hypothesis and a wet Moon. Earth and Planetary Science Letters,
622 487, pp.117-126.
623 Neal, C.R., Taylor, L.A., 1992. Petrogenesis of mare basalts: A record of lunar volcanism.
624 Geochimica et Cosmochimica Acta, 56, 2177-2211.
625 Ni, P., Zhang, Y., Chen, S., Gagnon, J., 2019. A melt inclusion study on volatile abundances in
626 the lunar mantle. Geochimica et Cosmochimica Acta, 249, 17-41.

627 O'Neill, H.St.C., 1991. The origin of the Moon and the early history of the Earth – a chemical
628 model. Part 1: The Moon. Geochimica et Cosmochimica Acta, 55, 1135-1157.
629 Paniello, R.C., Day, J.M.D., Moynier, F., 2012a. Zinc isotopic evidence for the origin of the Moon.
630 Nature, 490, 376-379.
631 Paniello, R.C., Moynier, F., Beck, P., Barrat, J.A., Podosek, F.A., Pichat, S., 2012b. Zinc isotopes
632 in HEDs: Clues to the formation of 4-Vesta, and the unique composition of Pecora Escarpment
633 82502. Geochimica et Cosmochimica Acta, 86, 76-87.
634 Pringle, E.A., Moynier, F., 2017. Rubidium isotopic composition of the Earth, meteorites, and the
635 Moon: Evidence for the origin of volatile loss during planetary accretion. Earth and Planetary
636 Science Letters, 473, 62-70.
637 Rhodes, J.M., Hubbard, N.J., 1973. Chemistry, classification, and petrogenesis of Apollo 15 mare
638 basalts. Lunar and Planetary Science Conference Proceedings, 4, 1127-1147.
639 Sarafian, A.R., John, T., Roszjar, J., Whitehouse, M.J., 2017. Chlorine and hydrogen degassing in
640 Vesta's magma ocean. Earth and Planetary Science Letters, 459, 311-319.
641 Schnare, D.W., Day, J.M.D., Norman, M.D., Liu, Y., Taylor, L.A., 2008. A laser-ablation ICP-
642 MS study of Apollo 15 low-titanium olivine-normative and quartz-normative mare basalts.
643 Geochimica et Cosmochimica Acta, 72, 2556-2572.
644 Sedaghatpour, F., Jacobsen, S.B., 2019. Magnesium stable isotopes support the lunar magma
645 ocean cumulate remelting model for mare basalts. Proceedings of the National Academy of
646 Sciences, 116, 73-78.
647 Sharp, Z.D., Shearer, C.K., McKeegan, K.D., Barnes, J.D., Wang, Y.Q., 2010. The chlorine
648 isotope composition of the Moon and implications for an anhydrous mantle. Science, 329, 1050-
649 1053.
650 Shearer, C.K., Sharp, Z.D., Burger, P.V., McCubbin, F.M., Provencio, P.P., Brearley, A.J., Steele,
651 A., 2014. Chlorine distribution and its isotopic composition in "rusty rock" 66095. Implications
652 for volatile element enrichments of "rusty rock" and lunar soils, origin of "rusty" alteration, and
653 volatile element behavior on the Moon. Geochimica et Cosmochimica Acta 139, 411-433.
654 Shearer, C.K., Elardo, S.M., Petro, N.E., Borg, L.E., McCubbin, F.M., 2015. Origin of the lunar
655 highlands Mg-suite: An integrated petrology, geochemistry, chronology, and remote sensing
656 perspective. American Mineralogist, 100, 294-325.
657 Sossi, P.A., Nebel, O., O'Neill, H.S.C., Moynier, F., 2018. Zinc isotope composition of the Earth
658 and its behaviour during planetary accretion. Chemical Geology, 477, 73-84.
659 Sossi, P.A., Moynier, F., 2017. Chemical and isotopic kinship of iron in the Earth and Moon
660 deduced from the lunar Mg-Suite. Earth and Planetary Science Letters, 471, 125-135.
661 Snyder, G.A., Taylor, L.A., Neal, C.R., 1992. A chemical model for generating the sources of mare
662 basalts: Combined equilibrium and fractional crystallization of the lunar magmasphere.
663 Geochimica et Cosmochimica Acta, 56, 3809-3824.
664 Spicuzza, M.J., Day, J.M.D., Taylor, L.A., Valley, J.W., 2007. Oxygen isotope constraints on the
665 origin and differentiation of the Moon. Earth and Planetary Science Letters, 253, 254-265.
666 Taylor, S.R., Taylor, G.J., Taylor, L.A., 2006. The Moon: a Taylor perspective. Geochimica et
667 Cosmochimica Acta, 70, 5904-5918.
668 Urey, H.C., 1947, The thermodynamic properties of isotopic substances. Journal of the Chemical
669 Society (London), 562-581.
670 van Kooten, E.M.M.E., Moynier, F. 2019. Zinc isotope analyses of singularly small samples (< 5
671 ng Zn): investigating chondrule-matrix complementarity in Leoville. Geochimica et
672 Cosmochimica Acta, 261, 248-268.

673 Wang, K., Jacobsen, S.B., 2016. Potassium isotopic evidence for a high-energy giant impact origin
674 of the Moon. Nature, 538, 487-490.
675 Wang, Z.Z., Liu, S.A., Liu, J., Huang, J., Xiao, Y., Chu, Z.Y., Zhao, X.M. and Tang, L., 2017.
676 Zinc isotope fractionation during mantle melting and constraints on the Zn isotope composition
677 of Earth's upper mantle. Geochimica et Cosmochimica Acta, 198, pp.151-167.
678 Wang, X., Fitoussi, C., Bourdon, B., Fegley, B., Charnoz, S., 2019. Tin isotopes indicative of
679 liquid–vapour equilibration and separation in the Moon-forming disk. Nature Geoscience, 12,
680 707-711.
681 Warren, P.H., Wasson, J.T., 1979. The origin of KREEP. Reviews of Geophysics, 17(1), pp.73-
682 88.
683 Warren P.H., Wasson J.T., 1980. Further foraging of pristine nonmare rocks: Correlations between
684 geochemistry and longitude. Proc. 11th Lunar Planet. Sci. Conf. 431-470.
685 Wimpenny, J., Marks, N., Knight, K., Rolison, J.M., Borg, L., Eppich, G., Badro, J., Ryerson, F.J.,
686 Sanborn, M., Huyskens, M.H., Yin, Q.Z., 2019. Experimental Determination of Zn Isotope
687 Fractionation During Evaporative Loss at Extreme Temperatures. Geochimica et
688 Cosmochimica Acta, 259, 391-411.
689 Wolf, R., Anders, E., 1980. Moon and Earth: compositional differences inferred from siderophiles,
690 volatiles, and alkalis in basalts. Geochimica et Cosmochimica Acta, 44, 2111-2124.
691 Zhu, M.-H., Artemieva, N., Morbidelli, A., Yin, Q.-Z., Becker, H, Wünnemann, K. 2019.
692 Reconstructing the late accretion history of the Moon. Nature, 571, 226–229.

693 **Figures and Figure Captions**

694

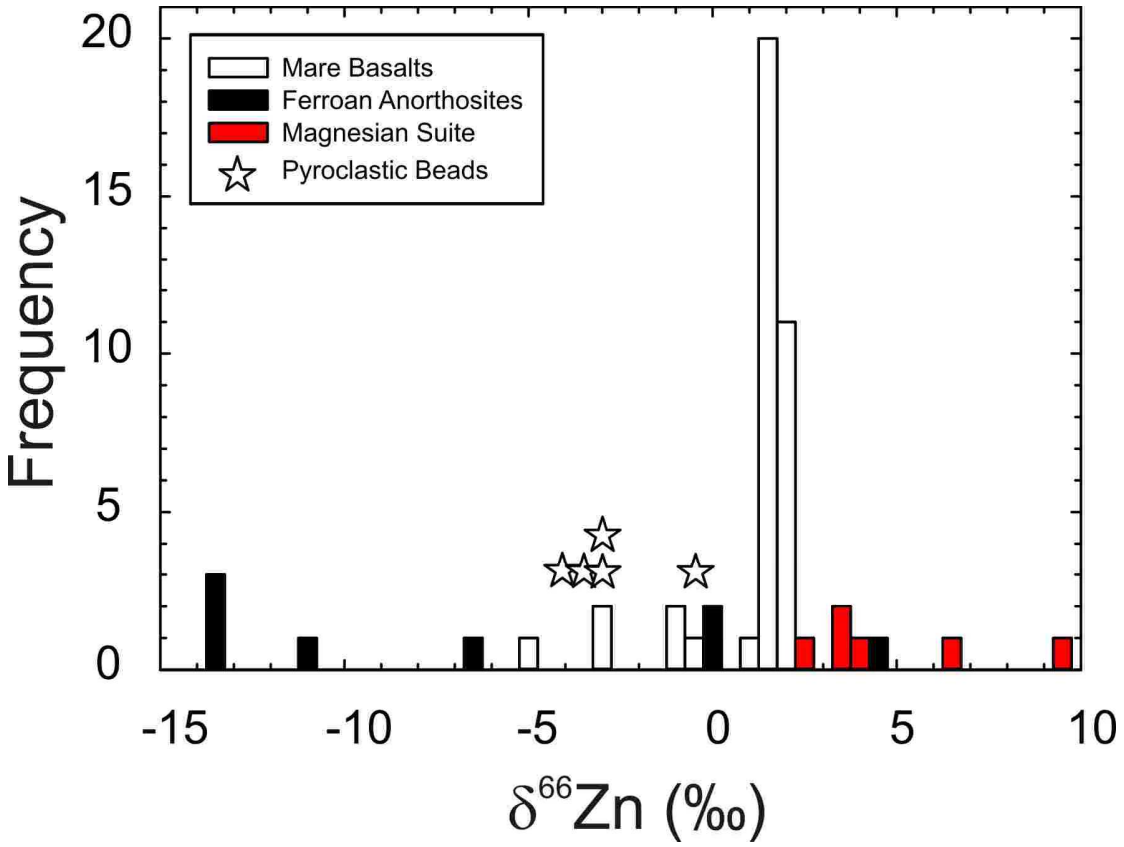

695

696 **Figure 1** – Histogram of zinc isotope compositions for lunar igneous samples. Data are from this
697 study (mare basalt meteorites and magnesian suite rocks), Moynier et al. (2006), Paniello et al.
698 (2012a) and Kato et al. (2015).

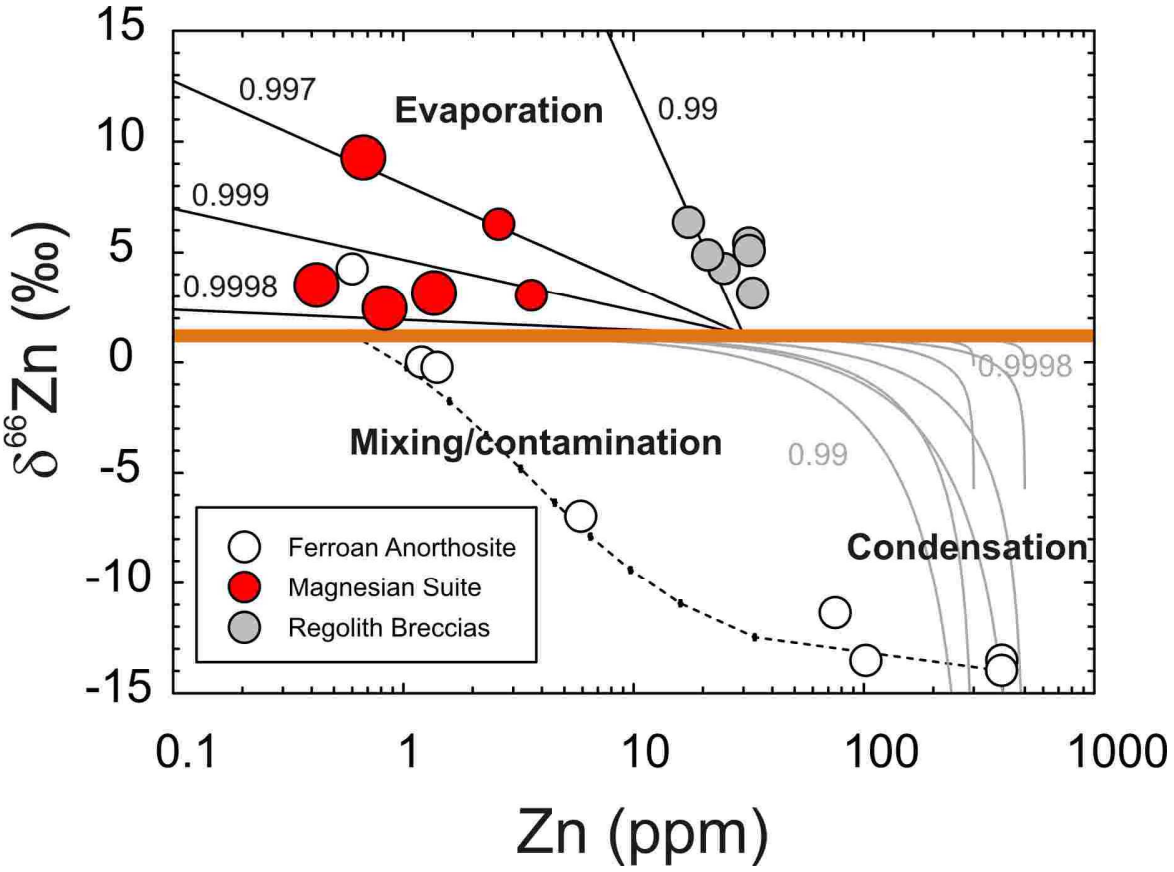

699

700 **Figure 2 –** Zinc isotope composition versus content for lunar crustal samples. Orange bar
701 represents the estimated range in δ^{66}Zn for the mare basalt source, from Paniello et al. (2012a).
702 Rayleigh distillation models of evaporation assume 30 ppm as the initial source composition, with
703 fractionation factors (α) from Day et al. (2017b), to more extreme values. Condensation models
704 represent sources with between 10-30 ppm initial Zn using the same fractionation factors. Mixing
705 and contamination line in increments of 10% models the effect of adding a Zn composition
706 observed in the 'Rusty Rock' 66095 with a pristine mare basalt composition and is after Day et al.
707 (2017a). Large symbols represent new data from the study, with published data from Herzog et al.
708 (2009), Kato et al., (2015) and Day et al. (2017a). Error bars are smaller than symbols.

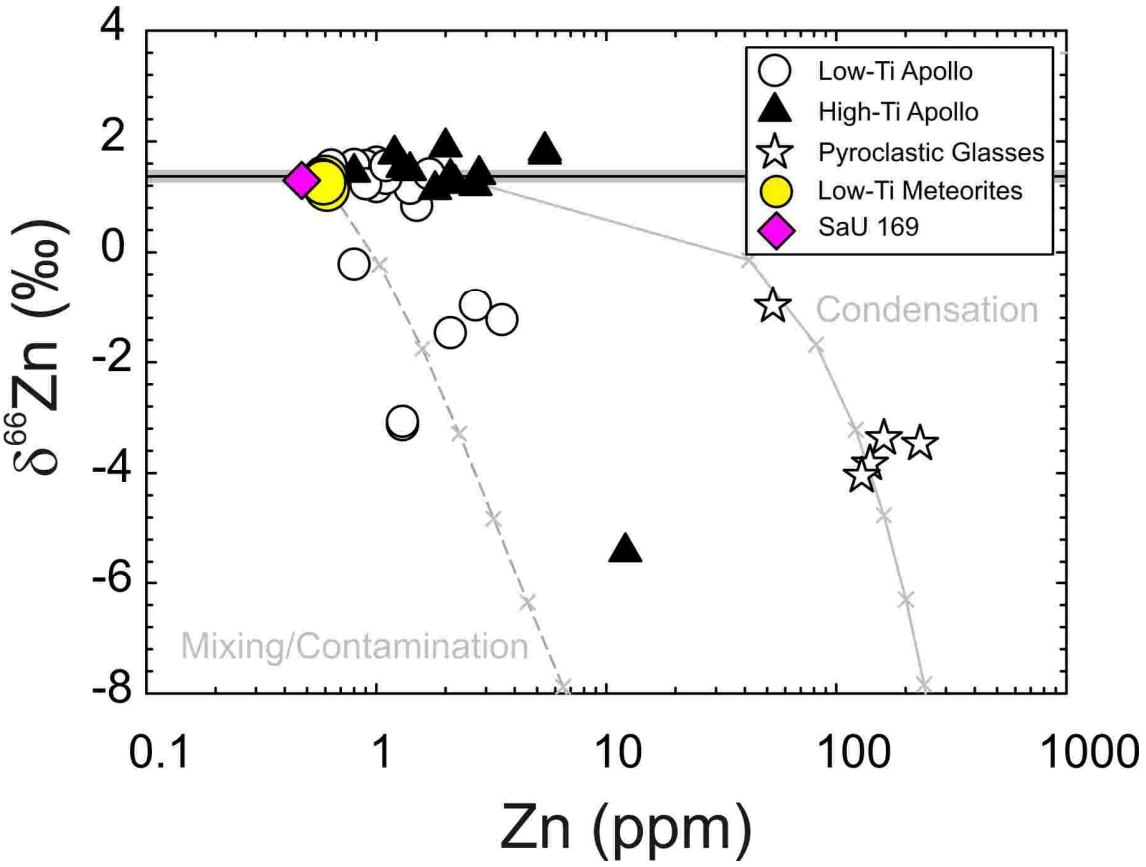

709

710 **Figure 3 -** Zinc isotope composition versus content for mare basalts and pyroclastic glasses. Solid
711 line and bar represent the estimated range in δ^{66}Zn for the mare basalt source, from **Table 2**.
712 Condensation and mixing/contamination models are the same as those calculated from Day et al.
713 (2017a) and Figure 2. Data are from this study (Low-Ti mare basalt meteorites and SaU 169),
714 Paniello et al. (2012a) and Kato et al. (2015). Error bars are smaller than symbols.

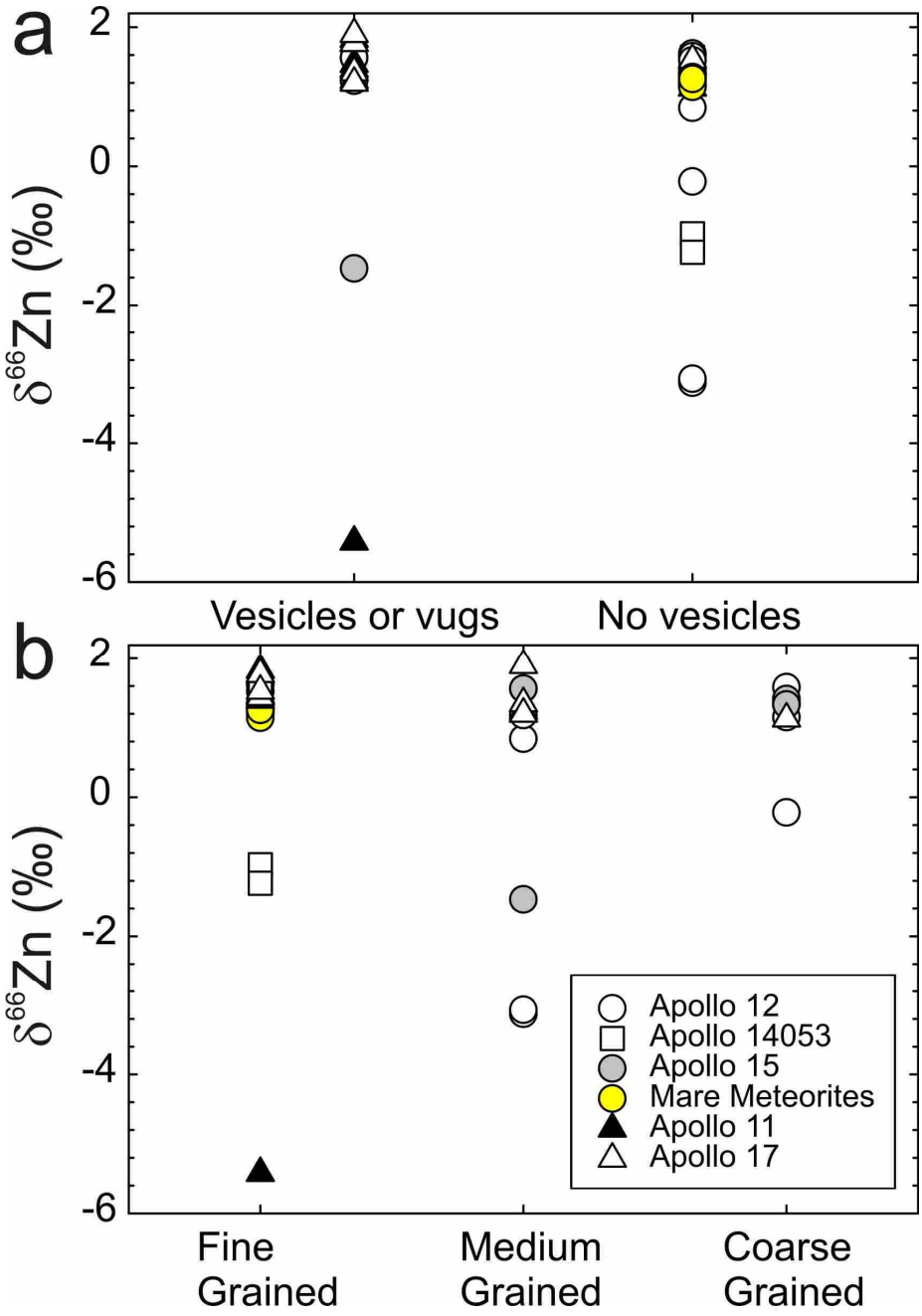

715

716

717 **Figure 4 –** Relationships of $\delta^{66}Zn$ for (a) vesiculated or vuggy versus non-vesicular mare basalts
718 and (b) versus mare basalt grain size. Data are given in **Table S1**.

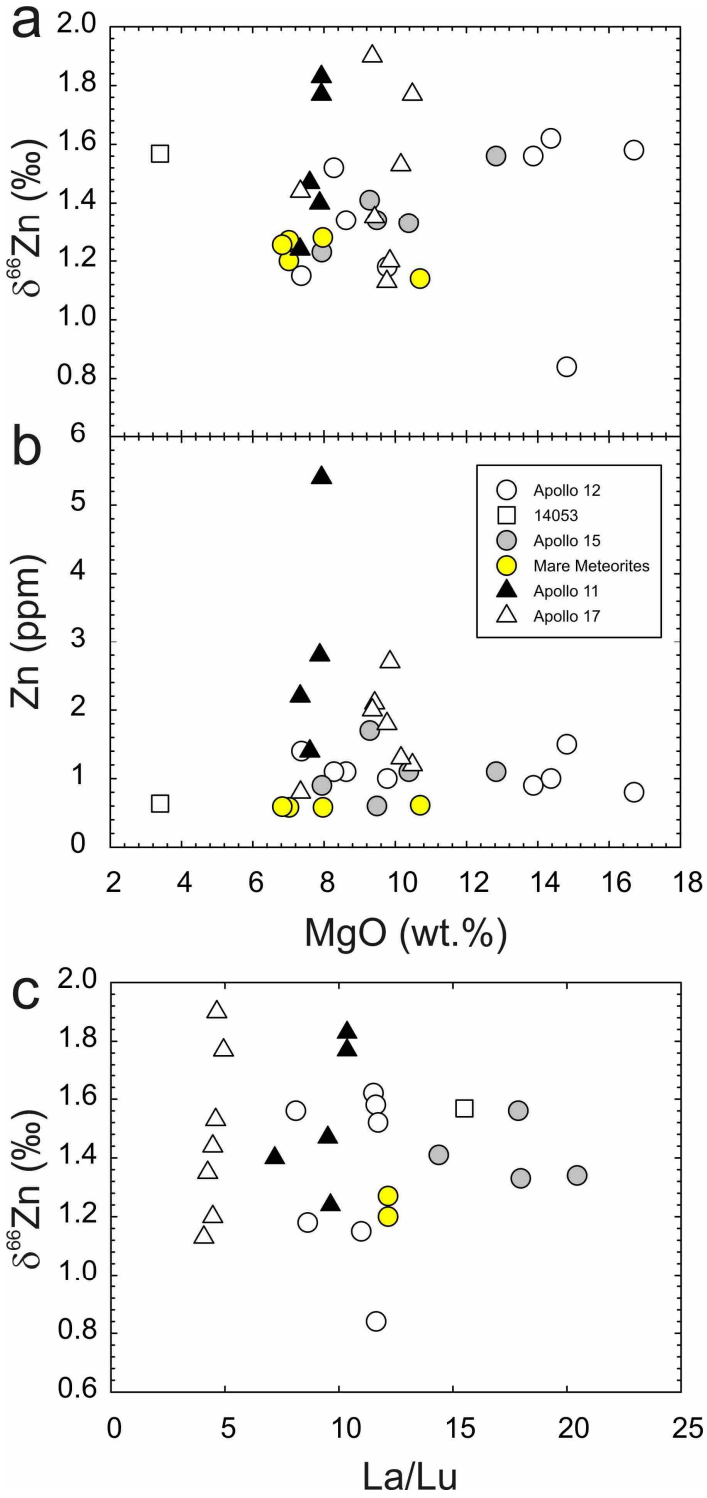

Figure 5 – Zinc isotope compositions (a) and abundances (b) for lunar mare basalts as a function of MgO content, and Zn isotopes versus La/Lu (c). Data for Zn are from this study, Paniello et al. (2012a), Kato et al. (2015), and for MgO content and La/Lu are from the lunar compendium and reported in **Table S1**. Error bars are smaller than symbols.

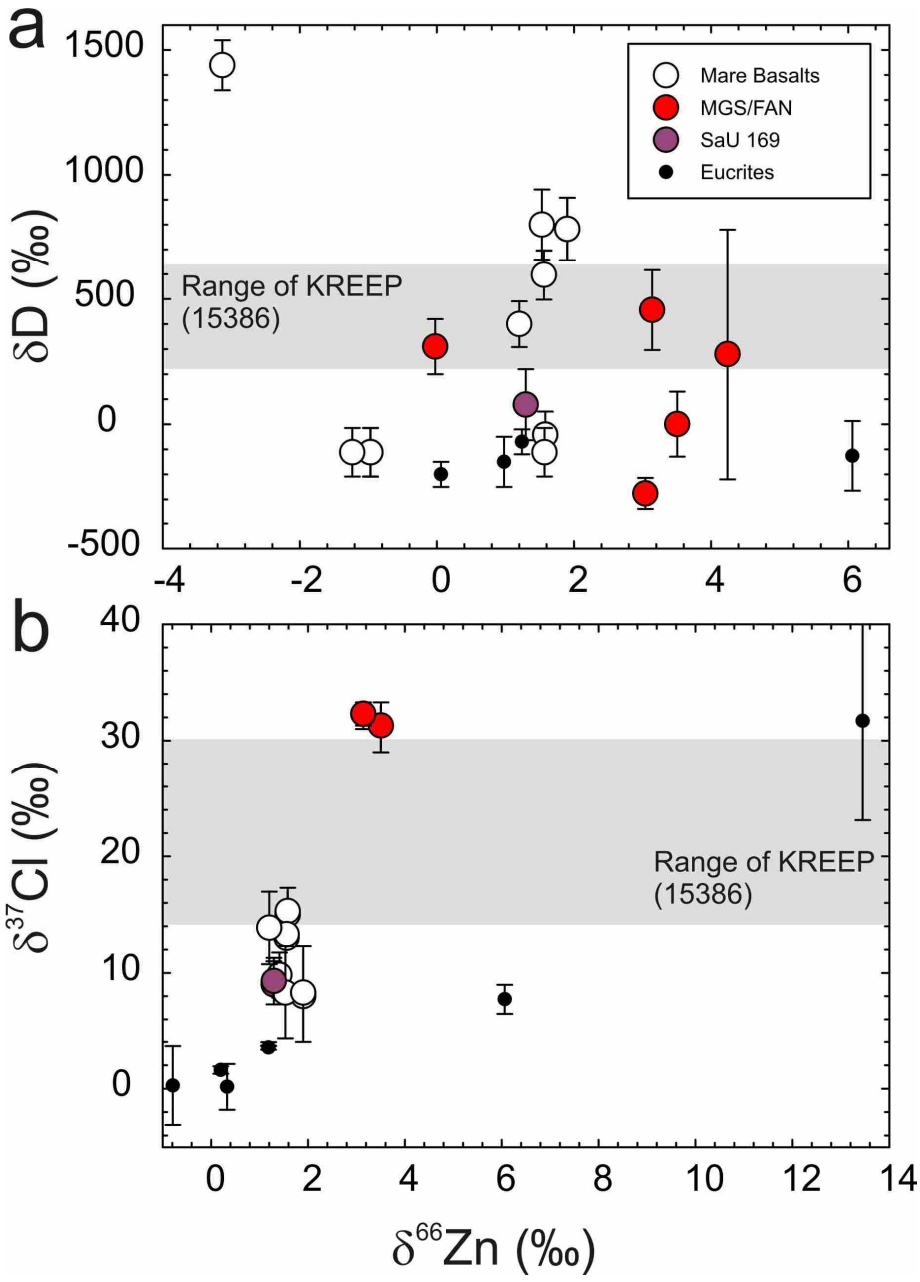

Figure 6 – Plots of (a) hydrogen and (b) chlorine versus zinc isotope composition for lunar samples and eucrite meteorites. Gray bar represents the hydrogen and chlorine isotope composition of KREEP basalt 15386; Zn isotope data has not been obtained for this sample. Zinc isotope data sources are the same as those for Figure 2, with lunar hydrogen and chlorine isotope data from the compilation in McCubbin et al. (2015), and H, Cl and Zn isotope data for eucrites from Paniello et al. (2012b), Sarafian et al. (2017) and Barrett et al. (2019) and reported in **Table S2**. Error bars are smaller than symbols, unless they are shown.

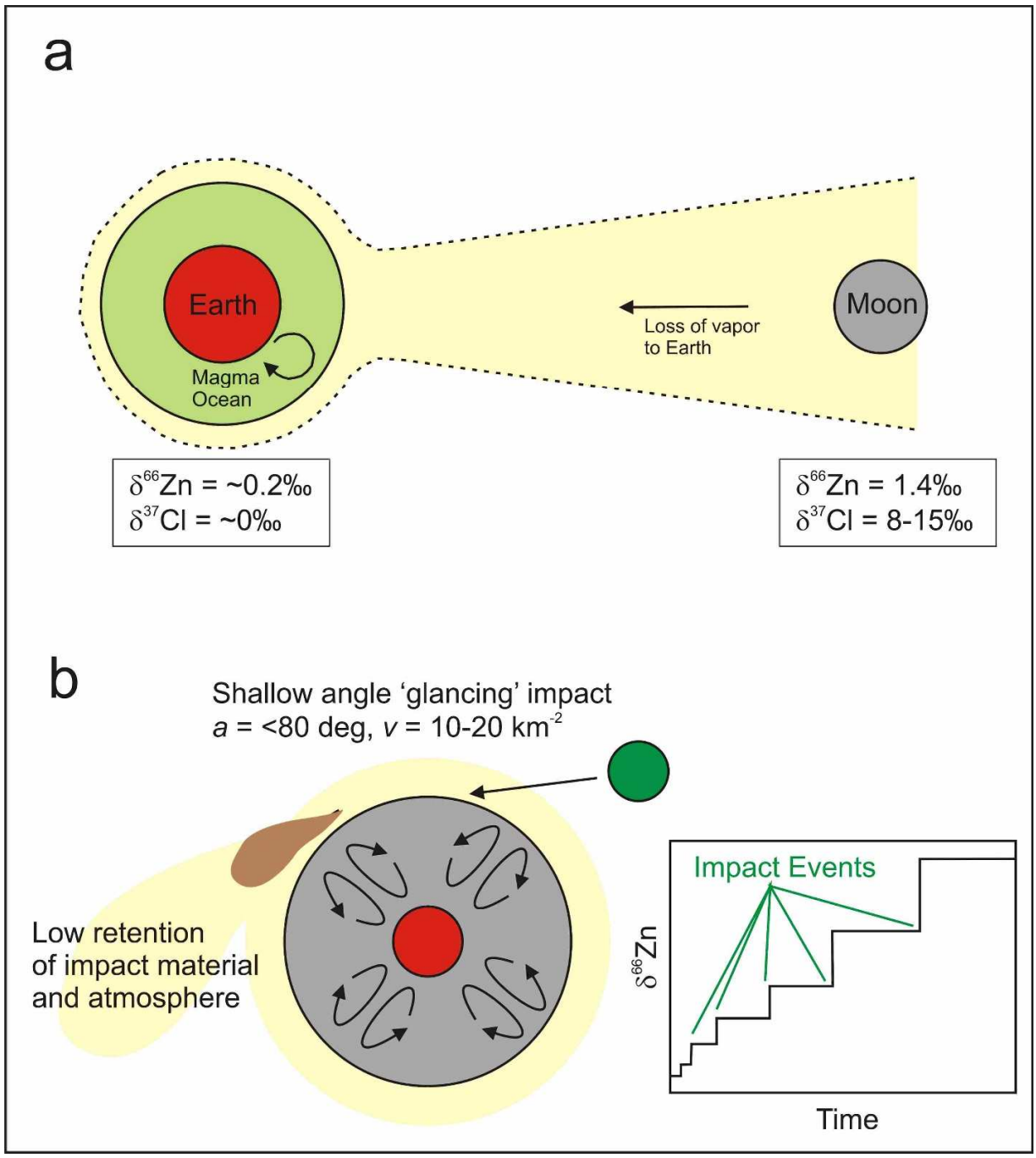

Figure 7 – Scenarios to explain the $\delta^{66}Zn$ and $\delta^{37}Cl$ of mare basalt mantle sources. In (a) the giant impact that created the Earth and Moon leads to volatile loss from the Moon, possibly to Earth or to space, resulting in a dichotomy in moderately volatile element abundances and isotopic compositions (c.f., Lock et al., 2018). In (b) impact erosion from glancing impacts to the Moon (cf. Zhu et al., 2019) lead to loss of impactor mass and of volatile elements. Multiple impacts result in progressive depletion in the volatile elements and preferential enrichment in the heavier isotopes of zinc (inset schematic).

Table 1: Zinc isotopes and abundances in mare basalt meteorites and Mg-suite rocks

Sample		Type	Zn ppm	δ^{66}Zn	2SD	δ^{66}Zn	2SD	δ^{66}Zn	2SD
78235, 156	Mg-Suite	Shocked Norite		3.40		5.30		6.90	
				3.61		5.66		7.3	
		Average	**0.42**	**3.51**	**0.30**	**5.48**	**0.51**	**7.10**	**0.57**
15455, 391	Mg-Suite	Norite CAN clast		9.23		14.27		18.74	
				9.31		14.52		18.89	
		Average	**0.67**	**9.27**	**0.11**	**14.40**	**0.35**	**18.82**	**0.21**
15445, 333	Mg-Suite	Norite (Clast B)		2.25		3.92		5.09	
				2.66		4.46		5.7	
		Average	**0.83**	**2.46**	**0.58**	**4.19**	**0.76**	**5.40**	**0.86**
76535, 186	Mg-Suite	Troctolite	**1.36**	**3.14**		**5.03**		**6.58**	
SAU 169	KREEP	Impact Melt		1.31		2.05		2.62	
		Breccia		1.28		1.91		2.52	
		Average	**0.47**	**1.30**	**0.04**	**1.98**	**0.20**	**2.57**	**0.14**
LAP 02205	Low-Ti Mare	Meteorite		1.28		1.76		2.56	
				1.26		1.98		2.56	
				1.27		1.86		2.55	
		Average	**0.58**	**1.27**	**0.02**	**1.87**	**0.22**	**2.56**	**0.01**
NWA 8632	Low-Ti Mare	Meteorite		1.16		1.65		2.39	
				1.12		1.69		2.23	
		Average	**0.61**	**1.14**	**0.06**	**1.67**	**0.06**	**2.31**	**0.23**
NWA 479	Low-Ti Mare	Meteorite		1.33		1.94		2.59	
				1.24		1.88		2.45	
				1.27		1.94		2.47	
		Average	**0.58**	**1.28**	**0.09**	**1.92**	**0.07**	**2.50**	**0.15**
NWA 4734	Low-Ti Mare	Meteorite		1.23		2.11		2.5	
				1.28		2.28		2.51	
		Average	**0.59**	**1.26**	**0.07**	**2.20**	**0.24**	**2.51**	**0.01**

Table 2: Zinc reservoir compositions in and on the Moon

	Zn ppm	2SE	δ^{66}Zn	2SE	n
Low-Ti Apollo Source(s)	1.1	0.2	1.37	0.12	14
Low-Ti Mare Meteorites	0.59	0.01	1.23	0.05	5
High-Ti Apollo Source(s)	2.4	0.9	1.50	0.15	12
Mare Sources			*1.40*	*0.20*	
KREEP	0.47	-	>1.3	-	1
Pristine FAN	0.60	-	>4	-	1
Mg-Suite	0.67	-	2.4 to 9.3	-	1
Condensate	300	100	-13.7	0.3	3
Impact Gardened Material	27	5	5.1	0.9	7